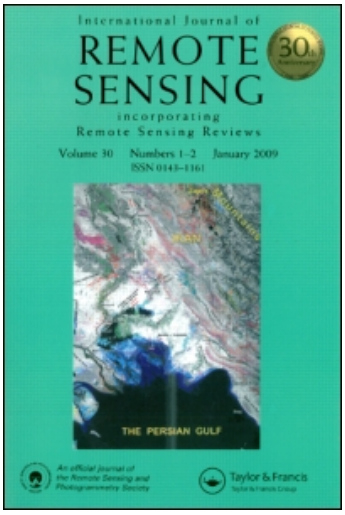

International Journal of Remote Sensing
Publication details, including instructions for authors and subscription information:
http://www.informaworld.com/smpp/title~content=t713722504

Integration of MODIS LAI and vegetation index products with the CSM-CERES-Maize model for corn yield estimation

Hongliang Fang[ab]; Shunlin Liang[a]; Gerrit Hoogenboom[c]
[a] Department of Geography, University of Maryland, College Park, MD, USA [b] NASA Goddard Earth Sciences Data and Information Services Center (GES DISC) employed by Wyle Information Systems, McLean, Virginia, USA [c] Department of Biological and Agricultural Engineering, University of Georgia, Griffin, GA, USA

Online publication date: 04 March 2011

To cite this Article Fang, Hongliang , Liang, Shunlin and Hoogenboom, Gerrit(2011) 'Integration of MODIS LAI and vegetation index products with the CSM-CERES-Maize model for corn yield estimation', International Journal of Remote Sensing, 32: 4, 1039 — 1065
To link to this Article: DOI: 10.1080/01431160903505310
URL: http://dx.doi.org/10.1080/01431160903505310

International Journal of Remote Sensing
Vol. 32, No. 4, 20 February 2011, 1039–1065

Taylor & Francis
Taylor & Francis Group

Integration of MODIS LAI and vegetation index products with the CSM–CERES–Maize model for corn yield estimation

HONGLIANG FANG†‡*, SHUNLIN LIANG† and GERRIT HOOGENBOOM§
†Department of Geography, University of Maryland, College Park, MD 20742, USA
‡NASA Goddard Earth Sciences Data and Information Services Center (GES DISC) employed by Wyle Information Systems, McLean, Virginia, USA
§Department of Biological and Agricultural Engineering, University of Georgia, Griffin, GA 20223, USA

(*Received 14 May 2009; in final form 20 November 2009*)

Advanced information on crop yield is important for crop management and food policy making. A data assimilation approach was developed to integrate remotely sensed data with a crop growth model for crop yield estimation. The objective was to model the crop yield when the input data for the crop growth model are inadequate, and to make the yield forecast in the middle of the growing season. The Cropping System Model (CSM)–Crop Environment Resource Synthesis (CERES)–Maize and the Markov Chain canopy Reflectance Model (MCRM) were coupled in the data assimilation process. The Moderate Resolution Imaging Spectroradiometer (MODIS) Leaf Area Index (LAI) and vegetation index products were assimilated into the coupled model to estimate corn yield in Indiana, USA. Five different assimilation schemes were tested to study the effect of using different control variables: independent usage of LAI, normalized difference vegetation index (NDVI) and enhanced vegetation index (EVI), and synergic usage of LAI and EVI or NDVI. Parameters of the CSM–CERES–Maize model were initiated with the remotely sensed data to estimate corn yield for each county of Indiana. Our results showed that the estimated corn yield agreed very well with the US Department of Agriculture (USDA) National Agricultural Statistics Service (NASS) data. Among different scenarios, the best results were obtained when both MODIS vegetation index and LAI products were assimilated and the relative deviations from the NASS data were less than 3.5%. Including only LAI in the model performed moderately well with a relative difference of 8.6%. The results from using only EVI or NDVI were unacceptable, as the deviations were as high as 21% and −13% for the EVI and NDVI schemes, respectively. Our study showed that corn yield at harvest could be successfully predicted using only a partial year of remotely sensed data.

1. Introduction

Reliable and timely prediction of crop yield is important for agricultural land management and policy making. Many studies have demonstrated the utilization of satellite data in crop yield estimation. Country-level crop yield estimation using

*Corresponding author. Now at: The State Key Laboratory of Resources and Environmental Information System (LREIS), Institute of Geographic Sciences and National Resources Research, Chinese Academy of Sciences (CAS), Beijing 100101, China. Email: Fanghl@lreis.an.cn

International Journal of Remote Sensing
ISSN 0143-1161 print/ISSN 1366-5901 online
http://www.tandf.co.uk/journals
DOI: 10.1080/01431160903505310

remote sensing data has been carried out operationally for more than two decades (MacDonald and Hall 1980). Vegetation indices calculated from Thematic Mapper (TM) data have improved the accuracy of ground wheat yield surveys through stratification of primary sampling units (Singh *et al.* 1992). Promising results have been obtained through the statistical relationship between satellite reflectance values or vegetation indices and crop yield (Thenkabail *et al.* 1992, Jiang *et al.* 2003, Kogan *et al.* 2005, Weissteiner and Kühbauch 2005). However, these methods are mainly empirical and they may work only for specific crop cultivars, a particular crop growth stage or environmental conditions at specific times.

Integration of remote sensing and crop growth simulation models has become recognized increasingly as a potential tool for crop growth monitoring and yield estimation (Abou-Ismail *et al.* 2004, Mo *et al.* 2005, Jongschaap 2006, Dente *et al.* 2008, Liang and Qin 2008). Several assimilation schemes with different degrees of complexity and integration have been developed during the last two decades (Maas 1988a, Delécolle *et al.* 1992, Moulin *et al.* 1998, Baret *et al.* 2000, Plummer 2000). Maas (1988a, b) initially reviewed different methods for combining a crop simulation model with radiometric observations (ground measurements or satellite data). Delécolle *et al.* (1992) generalized them into four methods: (1) directly using remotely sensed variables in the model; (2) updating state variables in the model; (3) re-initialization of the model; and (4) re-parametrization of the model. Re-parametrization is similar to re-initialization except that the model parameters are adjusted (Plummer 2000). Putting satellite products into crop growth models in the re-parametrization procedure corresponds to the highest degree of integration (Baret *et al.* 2000).

The essence of the data assimilation approach is to improve the initial parametrization of the crop growth model and augment simulation with the use of remotely sensed observations. Different researchers have used Leaf Area Index (LAI), spectral reflectance or vegetation indices as a control variable to adjust or to determine the optimal set of input parameters (e.g. Bach *et al.* 2001, 2003, Doraiswamy *et al.* 2003, Fang *et al.* 2008). Maas (1988a) and Dente *et al.* (2008) used remotely sensed LAI in the adjustment of model initial conditions to minimize the difference between model-predicted and remotely estimated LAI. Moulin *et al.* (1998) coupled a crop production model and a radiative transfer model, compared a simulated reflectance profile with a satellite-measured reflectance, and successfully re-tuned crop model parameters and initial conditions. Weiss *et al.* (2001) successfully assimilated the radiative transfer model SAIL and a crop growth model (STICS); simulated and measured reflectances agreed very well. Combining the process model (PROMET-V) with the canopy radiative transfer model Scattering by Arbitrarily Inclined Leaves (SAIL), Bach *et al.* (2001) obtained very good results for LAI, dry biomass and canopy height. De Wit (1999) integrated the World Food Studies (WOFOST) model (Boogaard *et al.* 1998) and satellite vegetation index data to retrieve wheat and sunflower conditions. Guérif and Duke (2000) also reported the usefulness of vegetation indices, especially for estimating the planting date and emergence parameters.

However, little work has been done to compare the performances by assimilating different satellite products, such as LAI and vegetation index. Doraiswamy *et al.* (2004) indicated that integrating remotely sensed LAI with a crop growth model has limitations and the data assimilation procedure needs further improvement. One major issue is related to the difficulty of obtaining an accurate LAI estimation from remotely sensed data. This limits the application of the data assimilation method at regional scales. Guérif and Duke (2000) compared the effect of spectral reflectance

and vegetation index and discovered that using a vegetation index was a better choice than spectral reflectance because the assimilation was very sensitive to variables such as soil reflectance and leaf optical properties in the canopy radiative transfer models.

In a previous study, Fang *et al.* (2008) developed an integrated crop simulation model, successfully estimating corn yield by integrating a crop growth model with the Moderate Resolution Imaging Spectroradiometer (MODIS) LAI products. This study extends that earlier work by assimilating both LAI and vegetation indices into the coupled crop growth and radiative transfer model in order to improve the estimation of crop yield on a county level. The effect of assimilating LAI separately and LAI and vegetation index synergistically was also studied. The next section presents the assimilation method, including crop model data preparation, remotely sensed data pre-processing, and different optimization schemes. The Cropping System Model (CSM)–Crop Environment Resource Synthesis (CERES)–Maize crop growth model and the Markov canopy reflectance model are presented. A sensitivity evaluation of the canopy reflectance model is introduced to determine the set of free parameters for the model. The results are analysed in the third section. Section four discusses the potentials and challenges of the data assimilation approach, followed by a conclusion section at the end of the paper.

2. Data assimilation method

The general methodology of the data assimilation method is illustrated in figure 1. Three steps were involved in this procedure.

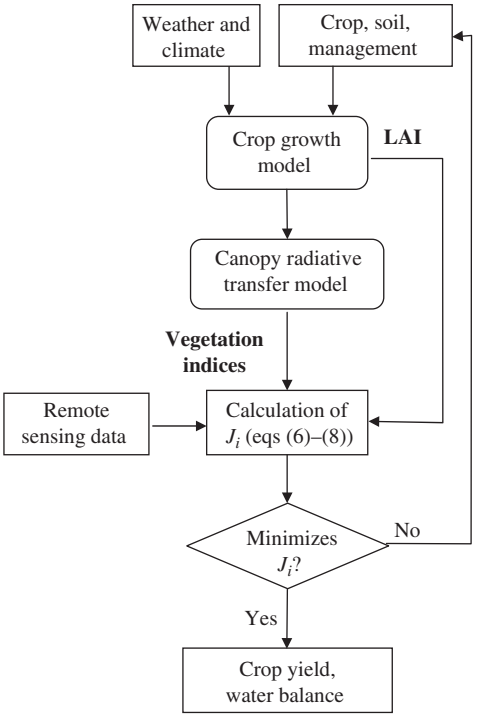

Figure 1. General methodology of the data assimilation approach integrating remote sensing data with crop growth and canopy reflectance models for crop yield estimation.

Table 1. Free parameters and their range in the coupled crop growth and canopy reflectance model.

Variables	Range
Crop growth model (CSM–CERES–Maize)	
Planting date (day of year)	98–158
Planting population (plants m^{-2})	6.0–7.5
Row spacing (cm)	75–90
Nitrogen amount in fertilizer (kg ha^{-1})	20–180
Canopy reflectance model (MCRM)	
Soil reflectance (red band)	0.02–0.5
Effective number of elementary layers in a leaf	1.0–3.0

1. Input data, such as crop characteristics, soil condition, management practice and weather information, were prepared in advance for the CSM–CERES–Maize model. A list of free variables is shown in table 1. With these input data, crop biophysical information (e.g. LAI) was generated by the crop growth model.
2. The parameters simulated by the crop model (e.g. LAI) and other ancillary information (e.g. soil reflectance) were used in the canopy reflectance model. Vegetation indices were calculated from the simulated reflectances.
3. The simulated vegetation indices and LAI were compared with the corresponding MODIS products, and residuals between the simulated and MODIS LAI or vegetation index were minimized by adjusting the input parameters in step 1. With the optimized set of input parameters, the model was executed to update the crop yield prediction.

2.1 *Material and models*

Our study area was the state of Indiana, USA, ranging from 37° 46′ N to 41° 46′ N and 84° 47′ W to 88° 6′ W. The topography of Indiana is characterized by vast flat plains in the northern two-thirds of the state and rugged hills in the southern. Indiana has a humid continental climate, with an annual precipitation of around 1000 mm. Corn and soybean are the two dominant crops. The average size of a farm is 240 ha. The prime planting period for corn is from late April to late May, while the typical harvesting period is from late September to early November. The statistical corn yield was obtained from the US Department of Agriculture (USDA) National Agricultural Statistics Service (NASS) reports for most counties in the state.

2.1.1 Crop growth and canopy reflectance models. The CSM–CERES–Maize model is a functional crop model that simulates growth, development and yield of corn under different weather, soil and management conditions (Jones *et al.* 2003). The CSM–CERES–Maize model used in this study was encompassed in the Decision Support System for Agrotechnology Transfer (Tsuji *et al.* 1994, Hoogenboom *et al.* 1999, 2004) package. The CSM–CERES–Maize model simulates phenological development, vegetative and reproductive plant development stages, partitioning of assimilates, growth of leaves and stems, senescence, biomass accumulation and root system dynamics. It has been used to predict grain yield and kernel numbers (Kiniry *et al.* 1997, Asadi and Clemente 2001, Lizaso *et al.* 2001, Tojo Soler *et al.* 2007), the effects of ground water and precipitation (Xie *et al.* 2001, O'Neal *et al.* 2002) and the effect of

increasing atmospheric carbon dioxide (Tubiello *et al.* 1999). The model has performed very well for predicting corn yield. For example, the relative errors are as low as 6.2% and 5%, as reported by Asadi and Clemente (2001) and Kiniry *et al.* (1997), respectively.

The Markov Chain Reflectance Model (MCRM) (Kuusk 1998) was used to simulate the reflectance at the top of the canopy. The Markov model simulates two-layer canopy reflectances at different solar illumination and viewing geometries (Kuusk 2001). In the MCRM model the canopy is assumed to be horizontally uniform above a horizontal ground surface. Leaf optical properties are simulated with the PROSPECT model (Jacquemoud and Baret 1990). The model was validated by the developers (Kuusk *et al.* 1997) and it performs very well in terms of accuracy and running time, and has been proved useful for crop canopy (Kuusk 1998, Jacquemoud *et al.* 2000, Fang and Liang 2003). Reflectances simulated by the Markov model for the top of canopy were used to compute the vegetation indices. The normalized difference vegetation index (NDVI) was calculated using the following equation:

$$\mathrm{NDVI} = \frac{\rho_{\mathrm{NIR}} - \rho_{\mathrm{R}}}{\rho_{\mathrm{NIR}} + \rho_{\mathrm{R}}}. \tag{1}$$

where ρ_{R} and ρ_{NIR} are surface reflectances of the red and near-infrared bands, respectively. The enhanced vegetation index (EVI) was calculated as:

$$\mathrm{EVI} = \frac{G(\rho_{\mathrm{NIR}} - \rho_{\mathrm{R}})}{\rho_{\mathrm{NIR}} + C_1\rho_{\mathrm{R}} - C_2\rho_{\mathrm{B}} + L}, \tag{2}$$

where ρ_{B} is the surface reflectance in the blue band, L is the canopy background adjustment and C_1 and C_2 are the coefficients of the aerosol resistance term. The coefficients used in the EVI calculation are $L = 1$, $C_1 = 6$, $C_2 = 7.5$ and G (gain factor) $= 2.5$ (Huete *et al.* 2002).

2.1.2 Evaluation of the canopy reflectance model. The number of free parameters is crucial in data assimilation. Sensitivity studies were conducted to identify the critical parameters for the crop growth model (Fang *et al.* 2008). An evaluation of the Markov model is indispensable to identify the optimal set of free parameters. Some studies have found that the optimization process is more robust if the number of free parameters is small (Kimes *et al.* 2000, Qin *et al.* 2008). Kimes *et al.* (2000) suggested that for radiative transfer model inversion, the number of free parameters that significantly impact the canopy reflectance ought to be minimal.

Among different algorithms for the radiative transfer model optimization, the genetic algorithm (GA) was used to determine the best set of free parameters. Genetic algorithm simulates the process of natural selection and evolutionary genetics. A detailed introduction of genetic algorithms can be found in Davis (1991) and Goldberg (1989). The general process is to adjust the radiative transfer model input parameters (genes in genetic algorithms) so that a simulated reflectance by the radiative transfer model agrees with the corresponding MODIS observation. Then some parameters that change less rapidly are fixed and the previous step is repeated until an optimal set of parameters is obtained. The advantage of using genetic algorithms is that it avoids the initial guess selection problem and provides a systematic scanning of the whole acceptable solution such that a global optimum solution could be reached.

The input parameters of the forward Markov model are summarized in table 2. The solar zenith angle (SZA) represents the values applicable to when the MODIS data were acquired. The leaf water content and leaf dry matter content (protein, cellulose

Table 2. Input parameters for the MCRM radiative transfer model.

Parameters	Symbol	Values
External parameters		
Solar zenith angle (°)	SZA	(from MODIS data)
Ångström turbidity factor	τ	0.1
Canopy structure parameters		
Leaf area index*	LAI	0–10.0
Leaf linear dimension/canopy height ratio	S_L	0.15
Markov parameter describing clumping*	S_Z	0.4–1.0
Leaf angle distribution*	LAD	0–90.0
Leaf spectral and directional properties		
Chlorophyll AB concentration (μg cm^{-2})*	C_{ab}	0–90
Leaf equivalent water thickness (cm)	C_w	0.01
Leaf protein content (g cm^{-2})	C_p	0.001
Leaf cellulose and lignin content (g cm^{-2})	C_c	0.002
Leaf structure parameter*	N	0.5–3.5
Soil spectral and directional properties (Price 1990)		
First weight of the Price function*	r_{s1}	0–1.0
Second weight of the Price function*	r_{s2}	–1.0–1.0
Third and fourth weights of the Price function	r_{s3}, r_{s4}	0.0

*Free parameter

and lignin) are from Jacquemoud *et al*. (1996). The sensitivity of the hot-spot parameter S_L (= 0.15) in the inversion is very low. Seven free parameters (or genes) were identified: LAI, S_z, leaf angle distribution (LAD), C_{ab}, N, $r_{s1,}$ and r_{s2}. Their effective ranges are displayed in table 2.

The simulated reflectances in the red and NIR bands were compared with MODIS reflectances. These two spectral bands were selected because they are the most frequently used bands in biophysical parameter retrieval (e.g. the MODIS LAI products) and they performed equally when compared to using more than two channels (Fang and Liang 2003, 2005). In this study, we started with testing all seven genes with the goal of finding the most sensitive ones. An example of the retrieved values for the seven parameters on day of year (DOY) 185 is shown in figure 2. Their mean, standard deviation (STD) and coefficient of variance (CV) values over the whole study area were also calculated. The Markov parameter describing clumping (S_z) was found to be the most stable variable in the study area, with a mean of 0.81 and the lowest CV (0.11). Other parameters, such as LAI and N, illustrate more heterogeneous conditions over the area. In this case, $S_z = 0.81$ was chosen to represent the general status of the study area and was fixed in the next iterations. In a similar fashion, a representative S_z value was derived for other days over the growing season (figure 3).

After S_z was fixed, a similar optimization procedure was applied to identify other less variable parameters. Starting with seven free parameters, S_z, LAD, N and C_{ab} were fixed sequentially with the number of genes reduced from 7 to 3. It is reasonable to assume that when the number of free parameters is decreased, the retrieved LAD, N and C_{ab} values may differ from those in the previous iteration. The times-series of the fixed values in figure 3 represent the general conditions of the study area in the assimilation experiments. The Markov parameter (S_z) ranges from 0.70–0.81

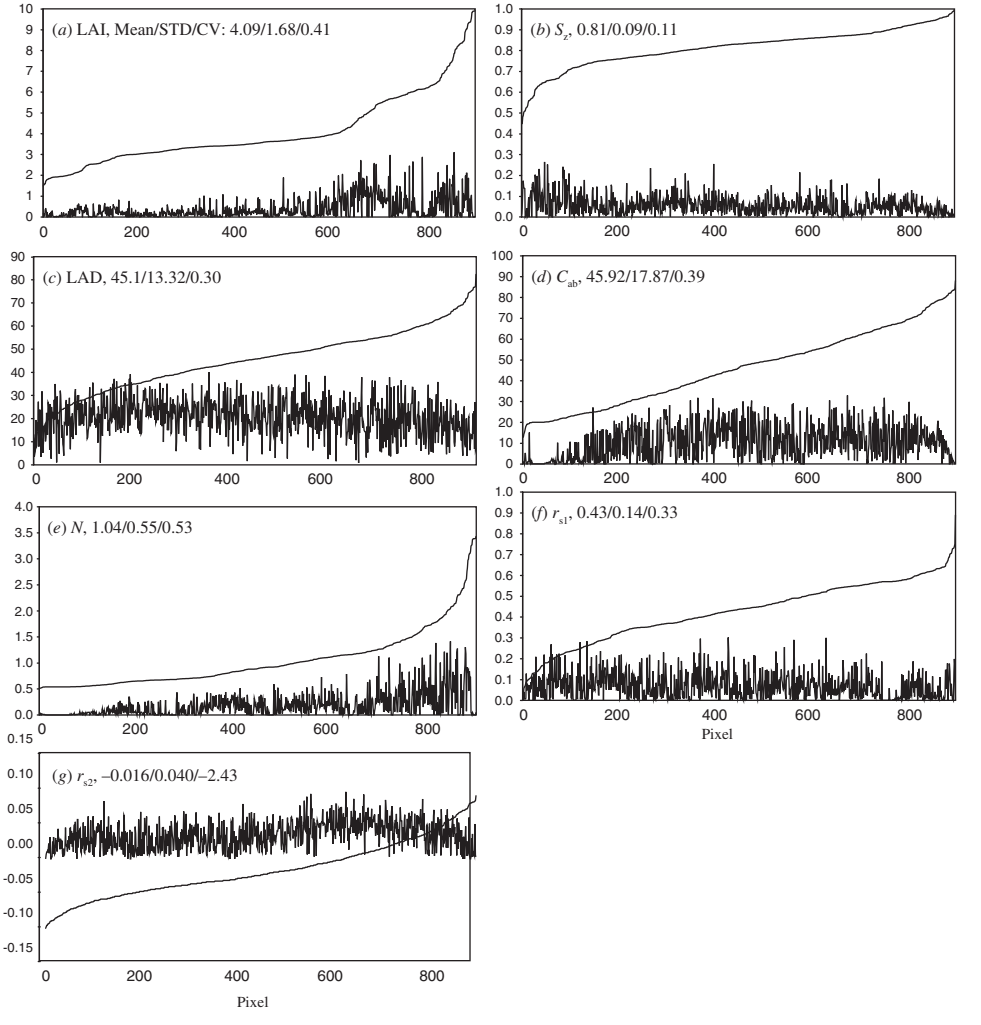

Figure 2. The sorted values of LAI, S_z, LAD, C_{ab}, N, r_{s1} and r_{s2} derived from the GA optimization method for all pixels in the study area on day 185. The abscissa represents the corn pixels in the study area. The thin lines show their corresponding standard deviation in the GA retrieval. The overall mean, standard deviation and coefficient of variation (CV) are also calculated.

over the growing season. A very stable value of LAD was observed when six genes were tested and thus leaf angle distribution (49.1°) was set to a constant value for the entire growing season. The retrieved leaf structure parameter (N) scatters between 1.0 and 3.0. The mean chlorophyll content (C_{ab}) showed a general increase from 7.5 μg cm^{-2} on day 137 to 54.0 μg cm^{-2} on day 193. After the maturity onset day (see §2.3.1 for the corresponding phenological stage), the retrieved C_{ab} became very unstable, ranging from 0.0 μg cm^{-2} to 90.0 μg cm^{-2} for the whole study area. LAI and soil reflectance (r_{s1} and r_{s2}) are the final parameters that were not fixed in the optimization process, indicating that they were very critical for the canopy reflectance simulation.

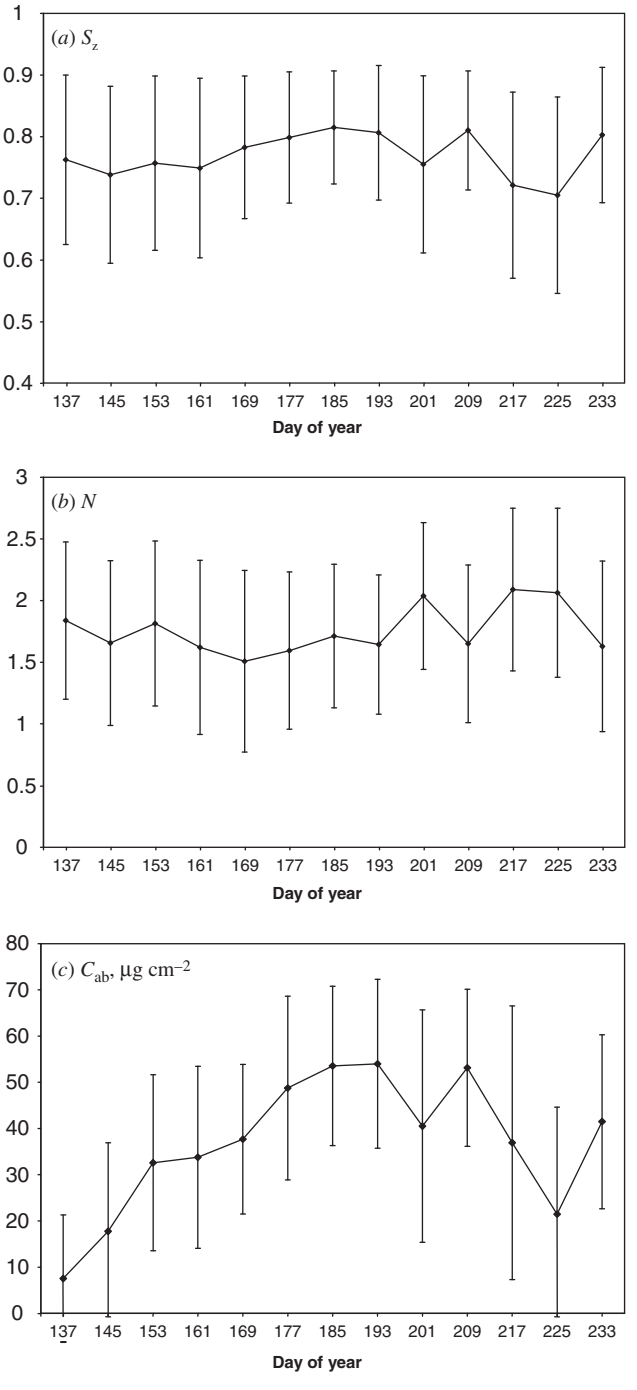

Figure 3. Series of the fixed S_z, N, and C_{ab} values in evaluating the MCRM model for the study area. The mean (dot) and standard deviation (lines) are also shown. S_z, N and C_{ab} are fixed using six, four and three genes, sequentially.

2.2 *Data preparation for model integration*

2.2.1 Input data for the crop growth model. Crop yield is influenced strongly by local cultivar characteristics, soil and weather conditions, and crop management. It may vary considerably in different fields and calendar years. The input parameters for the crop growth model include soil types, planting dates, planting rates and local weather data. For a local application (e.g. Guérif and Duke 2000), the initial conditions and the model parameters of crop leaf and soil optical properties are usually assumed to be known. Extending from a local to a large region requires automatic estimation of some of these parameters on a pixel basis.

Daily weather data, soil properties and crop ecology and management information are required to run the crop simulation model. Soil texture data from the USDA State Soil Geographic (STATSGO) database were used (http://www.ncgc.nrcs.usda.gov/branch/ssb/products/statsgo/index.html). Daily weather data were obtained from the North America Land Data Assimilation Systems (NLDAS) (http://ldas.gsfc.nasa.gov) because the data are spatially continuous with a high spatial resolution (1/8°). The soil and weather data were re-projected to a 1 km resolution.

Other crop growth studies have identified various parameters that are critical for LAI simulation. Bouman (1992) and Clevers *et al*. (1994) suggested using the 'light use efficiency' and 'maximum leaf area', while Maas (1988a) worked with the 'initial LAI'. Jongschaap (2006) experimented with the impact of field water content on simulated LAI. An earlier sensitivity analysis was conducted to identify the most critical parameters for crop model simulation (Fang *et al*. 2008). Some crop management variables, such as the corn cultivar type, planting date, planting population and row spacing, were found to be very critical for the execution of the CSM–CERES–Maize model (Fang *et al*. 2008). Pioneer cultivars (PC0003) represent the overwhelming majority of corn cultivars planted in Indiana and were used in the study. The planting date, planting population and row spacing were free variables and were estimated on a pixel basis (table 1). The USDA NASS reports provide the average planting date for each crop at the state level. The statistical planting date was used to determine their initial values for crop growth simulation (http://www. nass.usda.gov/in/annbul/0304/04weather.html).

The nutrient supply is represented by the application of nitrogen, which was set as a free variable. The date of nitrogen application was set to the same date as the planting date.

An initial parametrization was conducted by adjusting the CSM–CERES–Maize model to the USDA NASS corn yield at the state level. A list of values for all the free parameters was generated as a starting point for the pixel-specific calibrations in the optimization process.

2.2.2 Input data for the canopy radiative transfer model. For canopy biophysical and structural properties, such as the Markov parameter (S_z) and LAD, results from the above genetic algorithm optimization were applied (§2.1.2). Reference values from field measurements and remote sensing retrievals for similar corn fields were adopted for the leaf water and dry mater contents (table 2). The chlorophyll content of the leaf (C_{ab}) and the effective number of elementary layers inside a leaf (N) are crucial in the Markov model to simulate the leaf optical properties (Kuusk 1998). The current CSM–CERES–Maize model does not treat leaf chlorophyll content as an output even though the chlorophyll content could be estimated based on a correlation with the leaf nitrogen amount (Bullock and Anderson 1998). In this study, the leaf

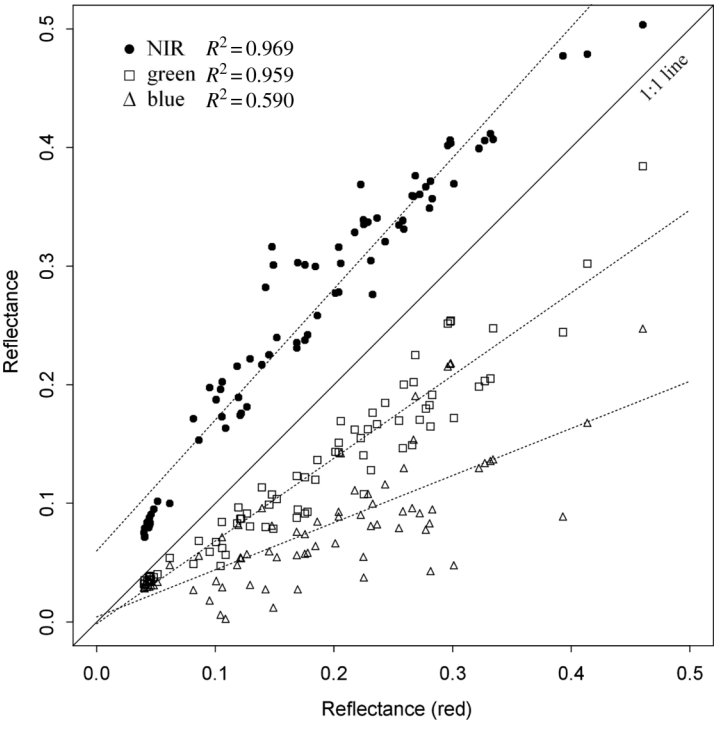

Figure 4. Analysis of the regression relationship of the soil near-infrared (NIR), green and blue band reflectances against the red band reflectance. The dashed lines are the regression lines for the NIR, green and blue bands, respectively.

chlorophyll content was fixed in order to focus on the effect of leaf structure and soil reflectance (table 1).

The soil reflectance (represented in the Price function) is an important parameter in the Markov model. In this study, an empirical method was developed to calculate the soil reflectance. The soil reflectance in the red band was set as a free variable between 0.02 and 0.50 (table 2). The soil reflectances for the blue, green and NIR bands were derived using the regression relationship (figure 4) created from the soil reflectance libraries provided by Daughtry (2001) and Dr J. Salisbury at the Johns Hopkins University (Jet Propulsion Laboratory 1998):

$$\begin{aligned} \rho_{\mathrm{B}} &= 0.397\rho_{\mathrm{R}} + 0.004 \\ \rho_{\mathrm{G}} &= 0.697\rho_{\mathrm{R}} - 0.002, \\ \rho_{\mathrm{NIR}} &= 1.105\rho_{\mathrm{R}} + 0.060 \end{aligned} \tag{3}$$

where ρ_{B}, ρ_{G}, ρ_{R} and ρ_{NIR} represent surface reflectances of the blue, green, red and near-infrared bands, respectively.

2.3 *Remotely sensed data and processing*

The quantity and timing of remote sensing data with regard to crop development will influence the assimilation performance (Moulin *et al.* 1998, Guérif and Duke 2000). Based on the same rationale from an earlier study (Fang *et al.* 2008), MODIS LAI,

NDVI and EVI products before the onset of senescence were used in this study. The standard MODIS LAI products are provided globally every eight days at a spatial resolution of 1 km (Justice *et al*. 1998, Myneni *et al*. 2002). Due to cloud and snow contamination, spatially and temporally complete LAI dataset are not available at the current stage. Therefore, the original MODIS LAI product was first processed with a method developed in this study (§2.3.1) before they were applied in the optimization process.

The MODIS NDVI and EVI products at a spatial resolution of 1 km and temporal resolution of 16 days were used in this study (Huete *et al*. 2002). These products are generated with a maximum value compositing (MVC) technique every 16 days (Huete *et al*. 2002). To calculate the vegetation index products, reflectances are calibrated to nadir view angle at a SZA representative of the observations (Justice *et al*. 1998). The vegetation index products have been well validated (Huete *et al*. 2002, Gao *et al*. 2003). We followed the same rationale above to select the vegetation index data. A total of seven values, starting on 8 May 2000 and ending on 12 August 2000 (day 129, 145 . . . 225) were used in the optimization process (§2.4).

2.3.1 MODIS LAI data processing. The essence of this LAI adjustment procedure is based on the common norm that crop LAI before the green-up onset should be nil. The LAI annual profile was first smoothed with the Savitzky–Golay (SG) filter (Savitzky and Golay 1964) to remove the temporal gaps and low quality pixels. The SG filter has been shown to be very helpful for smoothing of LAI. The hollow squares in figure 5(*b*) are the LAI points after SG smoothing.

The MODIS EVI products were used to model the vegetation phenological profile and determine the transition dates based on an approach developed by Zhang *et al*. (2003). This method uses a series of piecewise logistic functions fit to EVI to represent the intra-annual vegetation dynamics and identifies the phenological transition dates by the rate of change in curvature of the fitted logistic models. An example of the green-up and maturity onset dates generated by the piecewise logistic method is shown in figure 5(*a*) for a corn pixel in Indiana.

Since the LAI values before the green-up onset are zero, the Savitzky–Golay-filtered LAI was adjusted using a piecewise logistic function:

$$\mathrm{LAI}(t) = \frac{c}{1 + e^{a+bt}}, \tag{4}$$

where t is the time (day of year), LAI(t) is the LAI value at time t, a and b are fitting parameters, c is the maximum LAI value. Parameters a and b are calculated based on the LAI values at the green-up ($= 0$) and maturity onset dates. The solid squares in figure 5(*b*) are the adjusted LAI points for one corn pixel. In practice, we focused mainly on adjusting the LAI between the green-up and maturity onset dates. A total of 13 adjusted LAI values, starting on 16 May 2000 and ending on 20 August 2000 (days 137, 145 . . . 233) were used in the assimilation scheme. The extremely low LAI values before 16 May were discarded. After 20 August, the deviation between simulation and observation usually increases due to an increase in leaf senescence during the later stages of crop development (Jongschaap 2006).

2.4 *Model integration and optimization methods*

The crop growth and canopy reflectance models were coupled such that the crop biophysical parameters from the CSM–CERES–Maize model were used to drive

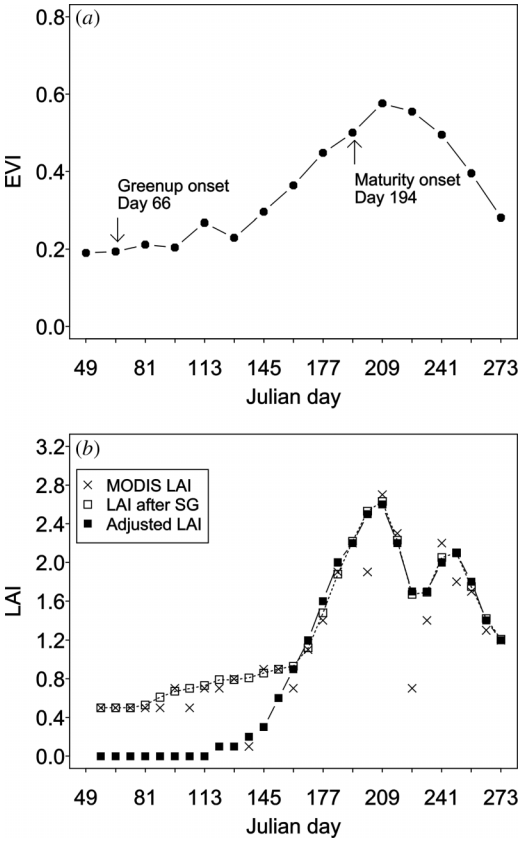

Figure 5. (*a*) A sample time-series of MODIS EVI data and the estimated phenological transition dates for a corn pixel in Indiana, 2000. (*b*) The original MODIS LAI (cross), the LAI after the SG filter (hollow square) and the adjusted LAI (solid square) based on the phenological dates from (*a*) and a piecewise logistic function in equation (4).

the Markov model. A general form of cost function J was constructed as (Liang 2004):

$$J(X(t_0)) = [X(t_0) - X_b]^T B^{-1} [X(t_0) - X_b] + \sum_{i=1}^{n} [H_i(X(t_i)) - Y_i]^T R_i^{-1} [H_i(X(t_i)) - Y_i], \quad (5)$$

where X_b is the background value (or first guess), $X(t_0)$ and $X(t_i)$ are the observed values at time t_0 and t_i, respectively, H is the crop model operator and Y_i are the observations. R and B are the observation and background error covariance matrices, respectively, and were set as unity here.

The cost function was based on the differences between the simulated and measured LAI using the conjugate direction optimization algorithm POWELL provided by Press *et al.* (1992). This method efficiently minimizes computing time and was used in this study. A simplified minimization was applied here to calculate the cost functions:

$$J_1 = \sum_{i=1}^{m} \mathrm{abs}\left[(\mathrm{LAI})_S(t_i) - (\mathrm{LAI})_M(t_i)\right]/(\mathrm{LAI})_M(t_i) \quad (6)$$

$$J_2 = \sum_{j=1}^{n} \mathrm{abs}\left[(\mathrm{VI})_S(t_j) - (\mathrm{VI})_M(t_j)\right]/(\mathrm{VI})_M(t_j) \quad (7)$$

$$J_3 = \frac{1}{m}\sum_{i=1}^{m} \mathrm{abs}\left[(\mathrm{LAI})_S(t_i) - (\mathrm{LAI})_M(t_i)\right]/(\mathrm{LAI})_M(t_i) + \frac{1}{n}\sum_{j=1}^{n} \mathrm{abs}\left[(\mathrm{VI})_S(t_j) - (\mathrm{VI})_M(t_j)\right]/(\mathrm{VI})_M(t_j), \quad (8)$$

where $\mathrm{LAI}_S(t_i)$, $\mathrm{LAI}_M(t_i)$ are the simulated and measured LAI at time t_i, respectively; VI_S, VI_M are the simulated and measured Vegetation Indices, respectively; m and n are the number of LAI and vegetation index values.

The optimization process starts from an initial parametrization and adjusts the free parameters in the coupled crop yield and radiative transfer model in order that the model gives LAI and/or vegetation index simulation in agreement with the MODIS observations. Table 3 shows an example of a typical optimization process for one pixel. The last column is the cost function calculated at different iterations based on equations (6), (7) and (8). Six model variables, four for the CSM–CERES–Maize (planting date, plant population, row spacing and nitrogen fertilizer amount) and two

Table 3. Adjustment of the free parameters in the optimization process.

No. iteration	Planting date (DOY)	Planting population	Row spacing (cm)	Nitrogen amount (kgha^{-1})	Soil red reflectance	Leaf structure	Cost function (J)
1	128	6.5	80	44	0.1	1.8	2.92
2	128	6.5	80	44	0.1	1.8	2.92
3	128	6.5	80	44	0.1	1.8	2.92
4	128.6	6.5	80	44	0.1	1.8	2.92
5	129.6	6.5	80	44	0.1	1.8	2.55
6	131.1	6.5	80	44	0.1	1.8	2.42
22	130	6.5	80	44	0.1	1.8	2.55
23	130	6.6	80	44	0.1	1.8	2.55
24	130	6.6	80	44	0.1	1.8	2.55
25	130	6.7	80	44	0.1	1.8	2.55
26	130	6.9	80	44	0.1	1.8	2.55
27	130	7.2	80	44	0.1	1.8	2.55
28	130	7.5	80	44	0.1	1.8	59731.61
29	130	7.2	80	44	0.1	1.8	2.55
30	130	7.3	80	44	0.1	1.8	2.55
385	157.5	7.5	90	56.9	0.5	3	0.84
386	157.5	7.5	90	56.9	0.5	3	0.84
387	157.5	7.5	90	56.9	0.5	3	0.84
Optimized value	157.5	7.5	90	56.9	0.5	3	0.84

The parameters are adjusted sequentially based on the cost function J value. Planting date is the first parameter to be adjusted (rows in iterations 1–6), followed by the planting population (rows in iterations 22–30) and others. The last row shows the final optimized value.

for the Markov model (red band soil reflectance and the effective number of elementary layers in a leaf) were adjusted and optimized sequentially based on the cost function. The last row shows the resultant optimized values for that pixel when the maximum number of iterations or the minimum merit function is achieved.

The simulated LAI or vegetation index values depend on the values of the free variables (e.g. planting date, see table 1) that are estimated by minimizing the cost function J. To compare the effect of using different control variables, five schemes were designed: S1 (LAI), S2 (EVI), S3 (NDVI), S4 (EVI+LAI) and S5 (NDVI+LAI). The first scheme was similar to our earlier work using LAI as the control variable (Fang *et al*. 2008), but different free variables were applied in this study. The cost function equations (6), (7), and (8) were applied for schemes S1, S2 and S3, and S4 and S5, respectively.

3. Results

The model was run on a daily time step for each corn pixel (1 km) in Indiana in 2000. Only pixels that had more than 80% corn were treated as 'pure' corn pixels and were processed with this methodology. In total, 871 'pure' corn pixels were identified in 2000 (Fang *et al*. 2008) based on the USDA cropland data layer (CDL) (http://www.nass.usda.gov/research/Cropland/SARS1a.htm).

3.1 *Crop yield*

A comparison of the estimated corn yield and NASS yield data for selected counties in Indiana, 2000 is presented in figure 6. USDA NASS has developed methods to assess crop growth and development from various sources of information, including several types of surveys of farm operators. NASS provides monthly projected estimates of crop yield and production. For the estimated yield, a total of 43 counties contains valid yield data by having at least 5 km^2 planted in corn ($\geq$5 pixels) within the county. The results from the five schemes are shown. The dashed line indicates the mean absolute bias between the estimated and measured yields. The best results are based on schemes with both vegetation index and LAI (S4 and S5), which have the lowest root mean square errors (RMSEs) and biases. When only vegetation index is used (S2 and S3), the results are unacceptable. Using only LAI (S1) generates moderately good results. Comparing the distribution of the estimated and NASS yields for all counties in 2000, the NASS county yields are mostly clustered between 8000 kg ha^{-1} and 10 500 kg ha^{-1}, while the simulated yield scatters between 5000 kg ha^{-1} and 15 000 kg ha^{-1}. The yield distribution of schemes S1, S4 and S5 is comparable to that of the NASS data, while the mean values of S2 and S3 are higher and lower, respectively, than the NASS data.

Table 4 compares the statistics obtained from the estimated and NASS yields. The best results are obtained from S5 using NDVI+LAI, with an estimated yield that is only 0.2% lower than the NASS data. The corn yield from S4 (EVI+LAI) gives very good results and the relative difference is 3.5%. In contrast, the results from S2 and S3 differ greatly from the measurements. The standard deviations from the estimated results are all higher than those of the NASS data. The schemes with only EVI or NDVI perform poorly. Scheme S2 (EVI) and S3 (NDVI) show the largest overestimation (20.8%) and underestimation (–13.2%), respectively. This phenomenon indicates the importance of LAI in the data assimilation process and that the incorporation of both LAI and vegetation index can improve crop yield prediction.

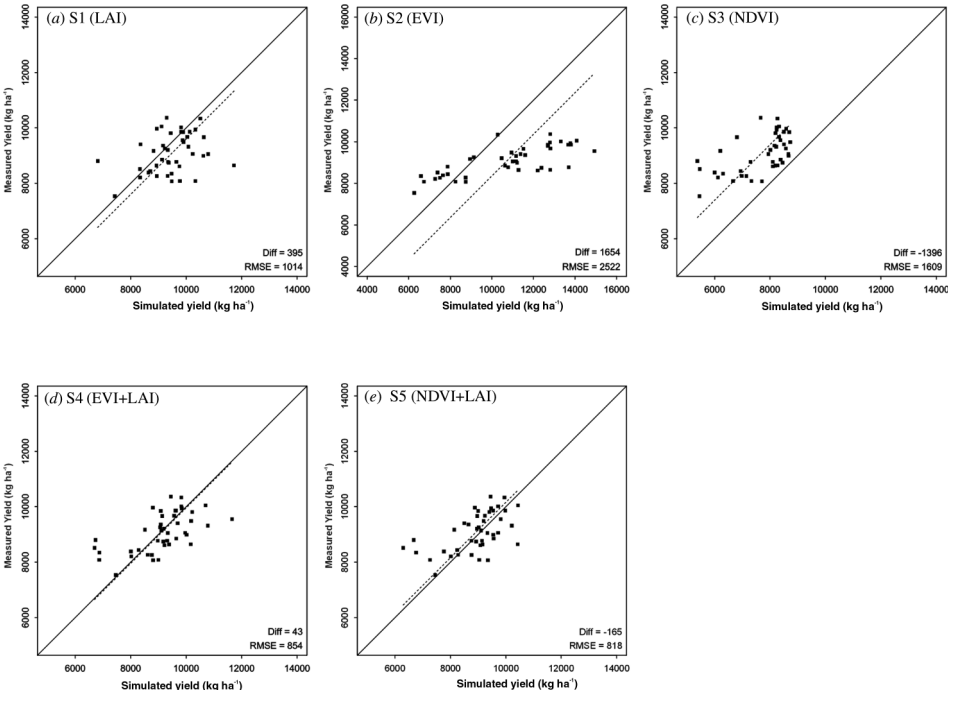

Figure 6. Comparison of the estimated corn yield and USDA NASS yield data for selected counties (43) in Indiana, 2000: (*a*) S1 (LAI); (*b*) S2 (EVI); (*c*) S3 (NDVI); (*d*) S4 (EVI+LAI); (*e*) S5 (NDVI+LAI). The abscissa and ordinate are the estimated and measured corn yield (kg ha^{-1}), respectively. The dashed line shows the mean offset indicated by 'Diff'. RMSE, root mean square error.

Figure 7 shows the spatial distribution of corn yield for different schemes on 11 July 2000 (Julian day 193). The corn yield was generated for 871 corn pixels in the state. It is clear that corn was grown mainly in the central counties of the state. The magnitude and spatial distribution in general agree with the NASS statistics. The Ohio River valley has the highest planting density and corn yield compared to other regions. The yield distributions of S4 and S5 are comparable to S1. For S2 and S3, discrepancies are seen in the eastern and northern parts of the state. The greatest deviation between the predicted and measured yields occurs for S2 (EVI only), which overestimates the corn yield, although the spatial pattern is in reasonable agreement with the observed

Table 4. Comparison of the estimated corn yield and NASS data in Indiana, 2000 (kg ha^{-1}).

		Estimated yields based on different schemes									
	NASS data	S1	(%)	S2	(%)	S3	(%)	S4	(%)	S5	(%)
Mean	9080	9857	8.6	10 967	20.8	7885	–13.2	9396	3.5	9060	–0.2
STD*	700	1228		2468		873		1405		1015	

Estimated yields are from five different schemes: S1 (LAI), S2 (EVI), S3 (NDVI), S4 (EVI+LAI) and S5 (NDVI+LAI). Their relative differences (%) with the NASS yield are also shown.
*STD, standard deviation.

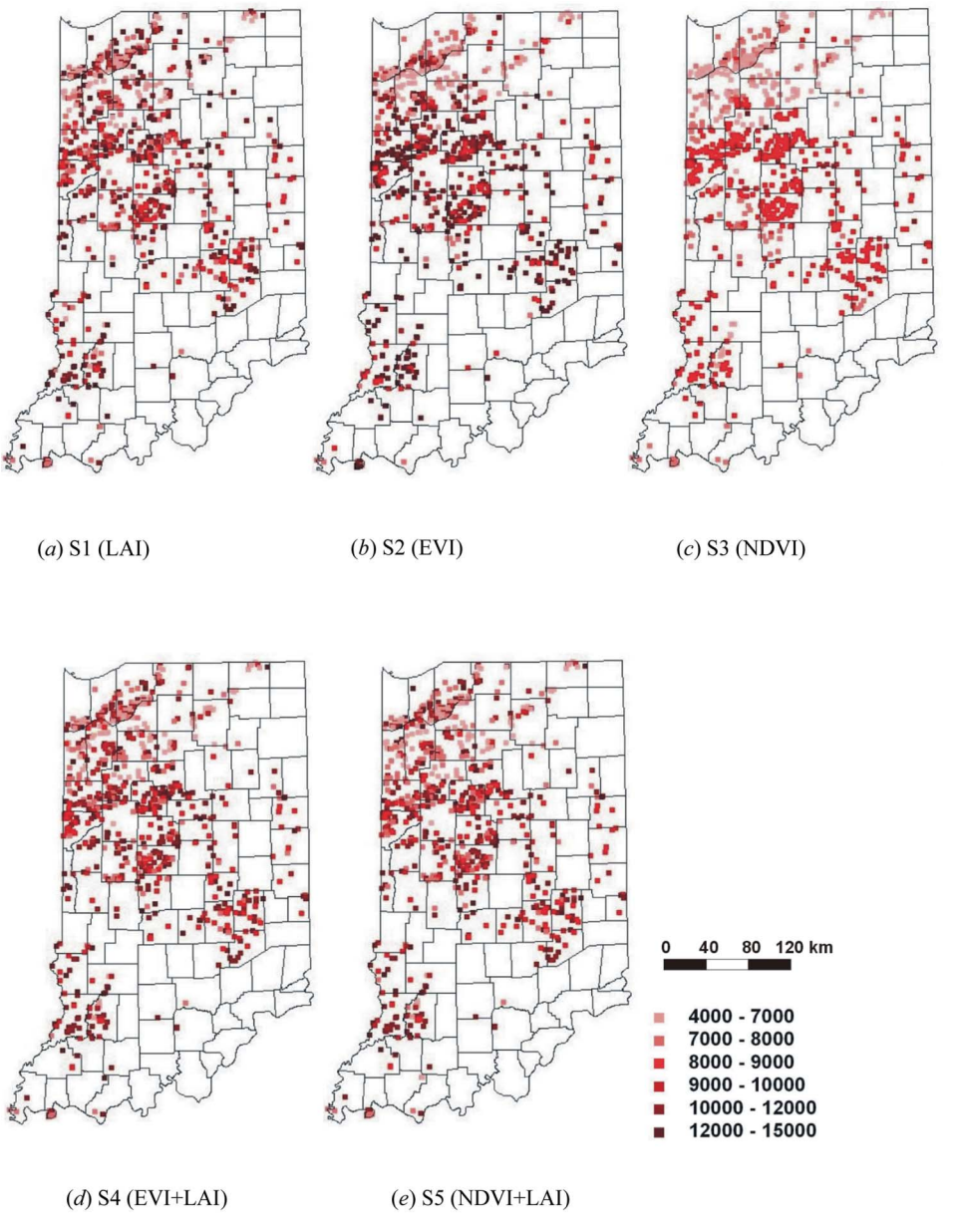

Figure 7. Spatial distribution of the estimated corn yields for Indiana, 2000 with five different schemes: (*a*) S1 (LAI); (*b*) S2 (EVI); (*c*) S3 (NDVI); (*d*) S4 (EVI+LAI); (*e*) S5 (NDVI+LAI). Unit: Kg ha^{-1}

values. In contrast, using NDVI only underestimates the corn yield, whereas its spatial pattern is quite similar to that when using EVI.

Using the adjusted LAI leads to an improved yield estimation when compared with a previous study using the original MODIS LAI (Fang *et al.* 2008). The mean difference in crop yield between the estimated and NASS decreased from 685 kg ha^{-1} using the

MODIS LAI to 395 kg ha^{-1} using the adjusted LAI. This indicates that the adjusted LAI could better characterize the crop growth status in the study area. Considering the uncertainties in the MODIS LAI products and in the coupled model, this level of yield agreement is very satisfying. In general, results from S1, S4 and S5 agree with the NASS data. Using both vegetation index and LAI demonstrated the best results.

3.2 *LAI estimated through data assimilation methods*

The current MODIS LAI products suffer from two problems: cloud contamination and temporal discontinuity (Myneni *et al.* 2002). The purpose of an eight-day composite is to eliminate cloud contamination, but it remains an issue in current MODIS LAI products (Myneni *et al.* 2002). Moreover, some studies require LAI with a higher temporal resolution. For example, Kang *et al.* (2003) used a linear interpolation to downscale from eight-day LAI to a daily unit for a greenness onset study. Interpolation and other mathematical fitting methods, while filling in missing days, would eventually change reliable values.

Although use of the MODIS daily surface reflectance could provide LAI at a daily time step, this advantage is constrained by daily cloud contamination and increased computing loads. Moreover, surface reflectance or its derivative (e.g. VIs) does not always correspond to an identical LAI value, but shows a statistical distribution that depends on the canopy physiological status (Myneni *et al.* 2002). In contrast, crop growth models can estimate LAI when no remote sensing products are available, especially during the early growth and senescence periods. Thus, it is feasible to monitor LAI and crop conditions all along the phenological cycle instead of only from isolated snapshot images.

The simulated mean LAI values from the five schemes are illustrated in figure 8. For comparison, the mean values of the MODIS LAI, the Savitzky–Golay-filtered LAI and the adjusted LAI are also displayed. All five schemes generate similar LAI values and profiles. In the CSM–CERES–Maize model, the estimation of LAI is based on the transformed dry matter from the absorbed solar energy, and the distribution of biomass among leaves, stems and roots. LAI relates mainly to the carbon balance in the crop simulation process and is more affected by crop type and weather conditions. In the re-initialization process for free variables, the simulated LAI values were automatically recalculated in the CSM–CERES–Maize model to fit the observed ones. Once the free variables are optimized, the simulated LAI profiles are similar among the different assimilation schemes (figure 8).

The seasonal phenology of the LAI is properly simulated by the model (figure 8). The modelled LAI and adjusted LAI match very well during the peak growing season and after maturity. The simulated LAI is within the standard deviation of the adjusted LAI (figure 8). Some deviations are evident during the green-up period. The seven-day difference (137, 145 ... 185) ranges from –0.09 to 0.95 and has a mean deviation of 0.31 between the simulated (S1) and adjusted LAI. However, the mean difference between the original MODIS LAI and simulated LAI (S1) ranges from 0.29 to 0.92, with a mean of 0.64. This phenomenon can be explained mostly by the obvious overestimation of the MODIS LAI products during the green-up period (Cohen *et al.* 2003, Fang and Liang 2005). This also reveals that the adjusted LAI could describe the crop growth status very well. The variation of both the MODIS LAI and the adjusted LAI is greater than that of the modelled LAI.

With the method developed in this study, we were able to generate a daily LAI map for the state of Indiana. Figure 9 displays the MODIS LAI product, the adjusted

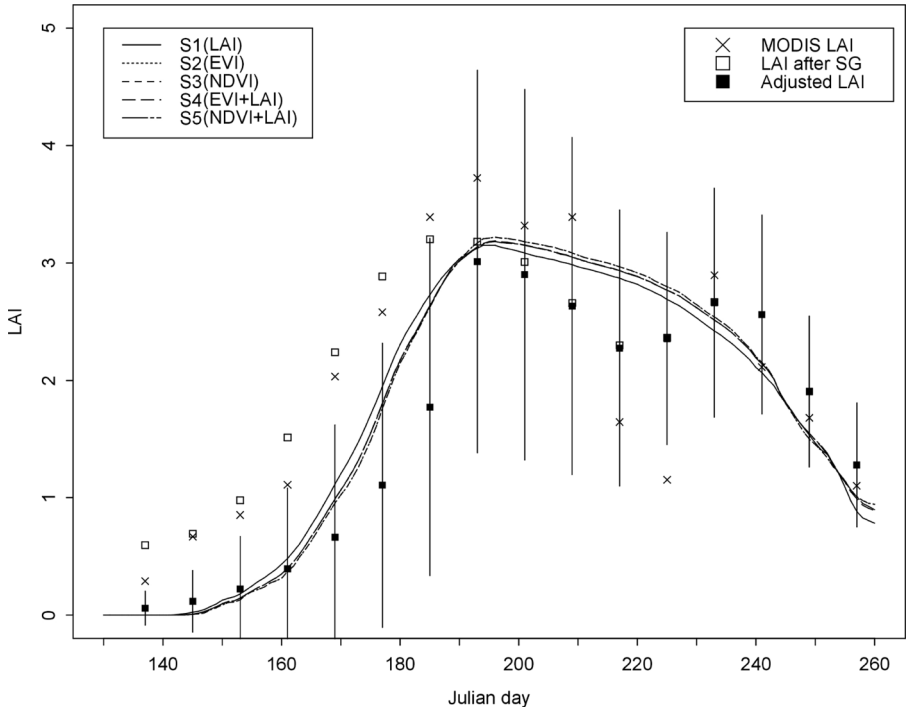

Figure 8. The simulated mean LAI for Indiana from the five schemes, 2000. Also shown are the original MODIS LAI (cross), the LAI after SG filtering (hollow square) and the adjusted LAI based on the piecewise logistic function (solid square). The segments are the standard deviation of the adjusted LAI over the state.

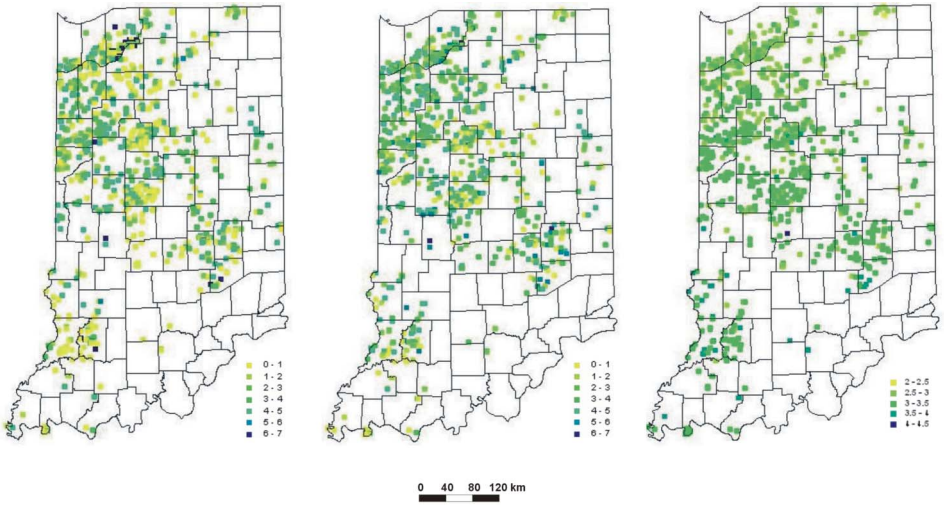

(*a*) MODIS LAI (*b*) Adjusted LAI (*c*) Simulated LAI

Figure 9. Comparison of (*a*) the MODIS LAI, (*b*) the adjusted MODIS LAI and (*c*) the simulated LAI from S4 (EVI+LAI) on day 193, 2000.

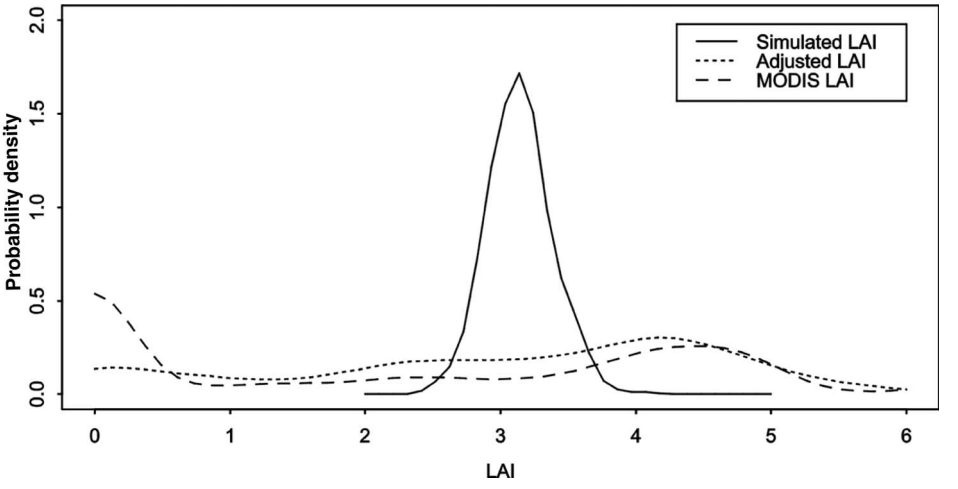

Figure 10. Comparison of the probability densities of the MODIS LAI, the adjusted LAI and the simulated LAI from S4 (EVI+LAI) on day 193, 2000.

MODIS LAI and the simulated LAI from S4 (EVI+LAI) on 11 July 2000 (DOY 193). The MODIS LAI product shows mixed LAI values evenly distributed across the state in July. Both the adjusted and simulated LAI values show a decreasing gradient between 1.0 and 2.0 from the west toward the east. Figure 10 shows the probability density of the modelled and MODIS LAI for the same day. For comparison, the temporally adjusted LAI is also displayed in figure 10. The adjusted LAI shows a very similar probability density as the MODIS LAI because of good observations for this eight-day period (figure 10). Visually, the adjusted LAI (figure 9(*b*)) is smoother than the original MODIS LAI (figure 9(*a*)) because the adjusted LAI enhances the low-LAI pixels (< 1) in central and southern Indiana and reduces some higher LAI pixels (> 6). The MODIS LAI shows a distribution plateau around 4.0–5.0. In contrast, the simulated LAI is concentrated around 2~4, with a peak at 3.0 (figures 9(*c*) and 10). Unlike the simulated LAI, the MODIS LAI values spread between 0 and 6. This is understandable because of the differences in algorithms, estimation assumptions and pixel unmixing methods.

3.3 *Vegetation indices*

Figure 11 shows the temporal profile of the simulated mean EVI (*a*) and NDVI (*b*) for the entire study area. For comparison, the state of Indiana's mean MODIS EVI and NDVI are also shown with dots (mean) and line segments (standard deviation). Figure 12 compares the probability density of the modelled and MODIS vegetation indices on 11 July 2000 (DOY 193).

Seven vegetation index values from the green-up to the peak growth period are compared (figure 11). After day 225, the vegetation index decreases. For the study period, the simulated EVI is lower than the NDVI. This is also observed for the MODIS vegetation index products. The highest simulated EVI and NDVI are observed at 0.68 and 0.90 for days 193 and 209, respectively (figure 11). Both S2 and S4 provide EVI as an intermediate variable. It is noted that the two EVI profiles from the two schemes are nearly identical (figure 11(*a*)). Likewise, S3 and S5 provided

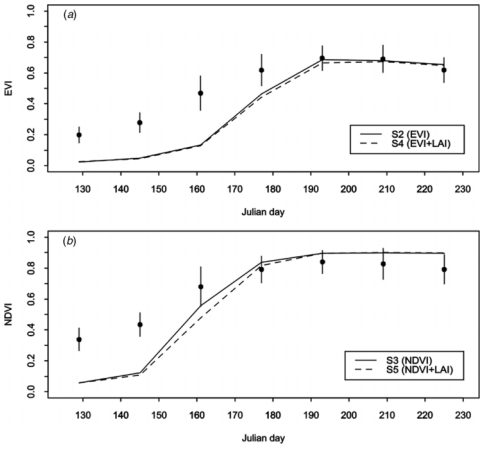

Figure 11. The simulated seasonal VIs for Indiana, 2000: (*a*) EVI from S2 and S4; (*b*) NDVI from S3 and S5. The points and segments are the mean and standard deviation of the MODIS EVI (*a*) and NDVI (*b*) products over the state.

very similar NDVI profiles (figure 11(*b*)). Among the seven days, the simulated vegetation indices agree very well with the MODIS vegetation index for the last four days (177, 193, 209 and 225). For three other days (129, 145 and 161), the MODIS vegetation index is higher than the simulated vegetation index. For these three days, the average deviations between the modelled and observed vegetation indices are 0.248 for EVI and 0.254 for NDVI, respectively. Like the MODIS LAI, the MODIS vegetation index values before emergence (e.g. day 129) may have a large variation resulting from a mixture of crop and soil at the surface (Huete *et al*. 2002). The standard deviation of the MODIS vegetation index is higher than those of the simulated ones, indicating that the MODIS vegetation index is more variable for Indiana. This is also illustrated by the probability density graph in figure 12.

The spatial distribution of the simulated EVI agree with the MODIS EVI except for a few isolated higher values (> 0.9). The same phenomenon is observed for the modelled NDVI and MODIS NDVI. The range of the simulated values is very similar to that of the observed ones, although the latter is more scattered. The simulated EVI distribution peak is at 0.724, compared to 0.714 for MODIS EVI (figure 12). For the simulated NDVI, there is a density peak at around 0.897, higher than that of the MODIS NDVI (0.857). The distribution of the MODIS vegetation index is more similar to a normal distribution, while the modelled ones are more clustered.

4. Discussion

4.1 *Practical application of the data assimilation approach*

With the coupled crop growth and canopy reflectance model, the seasonal corn yield was successfully estimated with only a partial year of remotely sensed data before senescence onset. In this study, MODIS LAI before 20 August 2000 (day 233) and vegetation index data before 12 August 2000 (day 225) were used to predict the end-of-season corn yield. In the study area, corn harvest usually happens from late September to early November. Spatial distribution information about crop yield

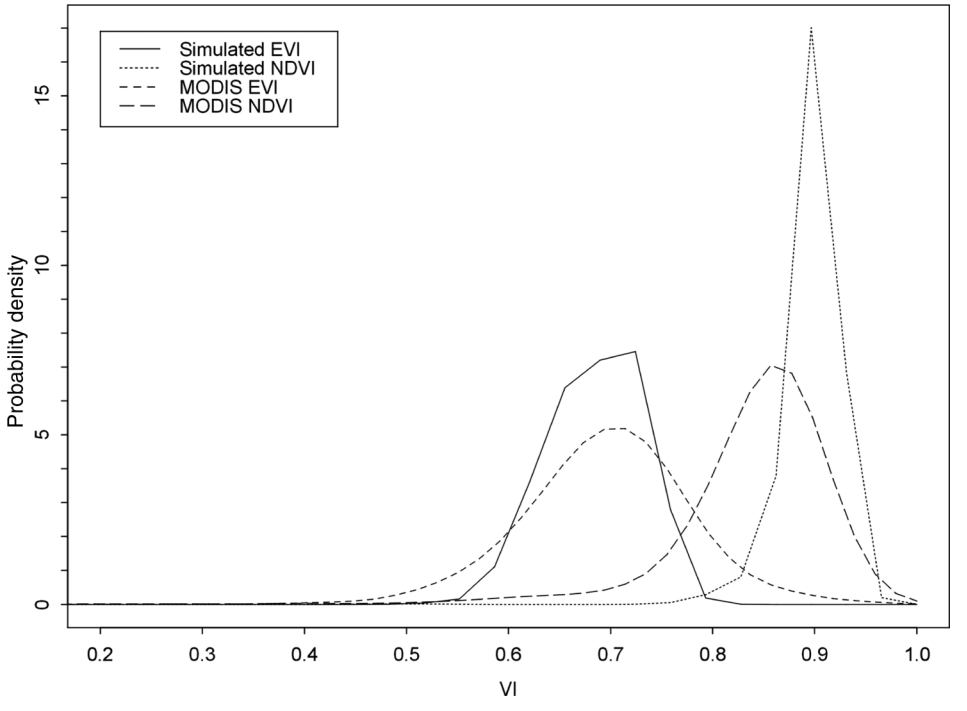

Figure 12. Comparison of the probability densities of the MODIS EVI and NDVI products with that of the simulated EVI and NDVI from S2 (EVI) and S3 (NDVI), respectively, on day 193, 2000.

was also obtained by this method. The data assimilation approach has great potential for operational corn yield estimation for other seasons.

One of our goals is to compare the effect of using LAI and vegetation index in data assimilation. The results indicate that LAI showed moderately good results while best results were obtained when both LAI and vegetation indices were used as the control variables. Using only NDVI significantly underestimated the corn yield while using only EVI over-predicted the yield. The inefficiency of using a vegetation index may be attributed to uncertainties in the radiative transfer model and the spatial variation of the MODIS products. Both schemes using NDVI (S3 and S5) predicted lower yields than those with EVI (S2 and S4). This might be due to soil background reflectance since it is not fully accounted for by NDVI.

In this study, daily LAI and vegetation index were generated through the CSM–CERES–Maize model. The MODIS LAI and vegetation index products reproduced the natural variation of the crop phenology satisfactorily. A new LAI adjustment method was developed to calibrate the original MODIS LAI based on the vegetation phenological information derived from the MODIS EVI product. The new LAI series consists of the adjusted LAI from the piecewise logistic function before maturity and the original MODIS LAI after maturity. The adjusted LAI proved to be very useful for the data assimilation study. When compared to using the original MODIS LAI, using the adjusted LAI data improved the corn yield estimation. Upon full validation, the simulated daily LAI and vegetation index data can complement the current MODIS products.

4.2 *Uncertainties and challenges*

There are several sources of uncertainty in the estimation of crop yield. For example, we assumed optimal growing and management conditions. However, management factors (e.g. a cultivar's genetic characteristics and use of fertilizers) and exceptional events (pests or flooding) will affect the predicted yield observed in farmers' fields. It is important to evaluate the model performance under high-yield conditions, as well as in environments that produce lower-yield levels under stress conditions to ensure a comprehensive assessment of model performance (Yang *et al*. 2004). USDA NASS yield statistics are designed to provide very accurate estimates at the state level, while in the assimilation model county-level yields are estimated and adjusted to sum to the state level. Note that these results are based on pixels at a 1 km resolution, while statistical yields are based on administrative regions.

The assimilation model would certainly benefit from better parametrization of the radiative transfer model. In this study, we fixed several parameters, such as canopy architecture, and leaf and soil optical properties. Better results may be obtainable with the use of more accurate parameter estimation for the leaf chlorophyll content, the total amount of equivalent water and dry matter (protein, cellulose and lignin). They may be obtained from the remote sensing methods separately and applied in the data assimilation process. For example, leaf chlorophyll content can be retrieved from high resolution remote sensing imagery (Fang *et al*. 2003). The leaf water content can be estimated from MODIS data through a radiative transfer model inversion method (Zarco-Tejada *et al*. 2003).

Potential uncertainties in the remotely sensed products need to be noted in such a data assimilation study. Some further improvements of the MODIS-derived LAI and vegetation index products are necessary, especially during the beginning of the growing season. This is also revealed in other similar studies (Adiku *et al*. 2006). In our study, the simulated LAI and vegetation index seasonal profiles showed that the MODIS LAI, EVI and NDVI products overestimated during the beginning of the season by about 0.64, 0.25 and 0.25, respectively.

Six model variables (table 1), four for the CSM–CERES–Maize model (planting date, plant population, row spacing and nitrogen fertilizer amount) and two for the Markov model (red band soil reflectance and the effective number of elementary layers in a leaf), were selected as free variables based on a series of sensitivity analyses. Different variable selection would affect the results. Since we focus on comparing the application of LAI and vegetation indices in the data assimilation process, a detailed sensitivity analysis considering other parameters should be performed in subsequent studies.

5. Conclusion

In this study, a data assimilation method was developed to estimate crop yield at the regional scale by assimilating MODIS LAI and vegetation index products into a coupled model consisting of the CSM–CERES–Maize crop growth model and the Markov canopy reflectance model. The assimilation method automatically tunes a set of input parameters until the difference between the MODIS LAI and vegetation index products and those simulated by the model is minimized. The final corn yield is estimated with the optimized input data.

By assimilating only a partial year of remotely sensed data we could effectively predict the seasonal crop yield one or two months before harvest. The estimated corn

yield over Indiana in 2000 agreed very well with the corn yield obtained from NASS statistics, both in spatial distribution as well as for the yield levels. The best results were obtained with a relative deviation less than 3.5% when both the LAI and EVI or NDVI were assimilated. When only one vegetation index was used, the bias was larger than 13%. Compared with using only LAI or only a vegetation index, a synergic use of LAI and vegetation index data makes the assimilated model more responsive to changes in the crop biophysical characters. The spatial variation of crop yield was found to be related to the scattering of the MODIS LAI and vegetation index products. With a proper model setting, the assimilation method described in this work is very promising for forecasting the long-term yield for other crop types in a larger region.

The soil, weather and crop parameter datasets developed for this study could provide useful guidelines for model applications in other regions. Several further studies can be foreseen. Regional hydrological information can be estimated by the assimilation approach in this study. Alternative optimization algorithms could be explored considering their computational efficiency and accuracy. Similar studies can be carried out for a different set of agricultural environment and canopy characteristics. More rigorous evaluation is necessary to investigate the model efficiency for various climatic and atmospheric conditions.

Acknowledgements

This work was supported by US Department of Agriculture (USDA) grant SCA58-1275-9-096. The authors would like to thank Dr Xiaoyang Zhang, Earth Resources Technology, Inc. for providing the phenology code. The daily weather data were distributed by the North America Land Data Assimilation Systems (NLDAS), located at the Goddard Space Flight Center, NASA (http://ldas.gsfc.nasa.gov/).

References

Abou-Ismail, O., Huang, J. and Wang, R., 2004, Rice yield estimation by integrating remote sensing with rice growth simulation model. *Pedosphere*, **14**, pp. 519–526.

Adiku, S.G.K., Reichstein, M., Lohila, A., Dinh, N.Q., Aurela, M., Laurila, T., Lueers, J. and Tenhunen, J.D., 2006, PIXGRO: A model for simulating the ecosystem CO2 exchange and growth of spring barley. *Ecological Modeling*, **190**, pp. 260–276.

Asadi, M.E. and Clemente, R.S., 2001, Simulation of maize yield and N uptake under tropical conditions with the CERES–Maize model. *Tropical Agriculture*, **78**, pp. 211–217.

Bach, H., Mauser, W. and Schneider, K., 2003, The use of radiative transfer models for remote sensing data assimilation in crop growth models. In *Precision Agriculture: Papers from the 4th European Conference on Precision Agriculture*, 15–19 June 2003, Berlin, Germany, J. Stafford and A. Werner (Eds), pp. 35–40 (Wageninger, The Netherlands: Wageninger Academic Publishers).

Bach, H., Schneider, K., Verhoef, W., Stolz, R., Mauser, W., Leeuwen, H., Schouten, L. and Borgeaud, M., 2001, Retrieval of geo- and biophysical information from remote sensing through advanced combination of a land surface process model with inversion techniques in the optical and microwave spectral range. In *8th International Symposium Physical Measurements & Signatures in Remote Sensing*, pp. 639–647 (France: Centre Paul Langevin, Aussois).

Baret, F., Weiss, M., Troufleau, D., Prevot, L. and Combal, B., 2000, Maximum information exploitation for canopy characterisation by remote sensing. *Aspects of Applied Biology*, **60**, pp. 71–82.

Boogaard, H.L., Diepen, C.A.v., Rötter, R.P., Cabrera, J.M.C.A. and Laar, H.H.V., 1998, *WOFOST 7.1; User's Guide for the WOFOST 7.1 Crop Growth Simulation Model and MOFOST Control Center 1.5* (Wageningen: DLO Winand Staring Centre).

Bouman, B.A.M., 1992, Linking physical remote sensing models with crop growth simulation models, applied for sugar beet. *International Journal of Remote Sensing*, **13**, pp. 2565–2581.

Bullock, D.G. and Anderson, D.S., 1998, Evaluation of the Minolta SPAD-502 chlorophyll meter for nitrogen management in corn. *Journal of Plant Nutrition*, **21**, pp. 741–755.

Clevers, J.G.P.W., Buker, C., Leeuwen, H.J.C.V. and Bouman, B.A.M., 1994, A framework for monitoring crop growth by combining directional and spectral remote sensing information. *Remote Sensing of Environment*, **50**, pp. 161–170.

Cohen, W.B., Maiersperger, T.K., Yang, Z., Gower, S.T., Turner, D.P., Ritts, W.D., Berterretche, M. and Running, S.W., 2003, Comparisons of land cover and LAI estimates derived from ETM+ and MODIS for four sites in North America: a quality assessment of 2000/2001 provisional MODIS products. *Remote Sensing of Environment*, **88**, pp. 233–255.

Daughtry, C.S., 2001, Discriminating crop residues from soil by shortware infrared reflectance. *Agronomy Journal*, **93**, pp. 125–131.

Davis, L., 1991, *Handbook of Genetic Algorithms* (New York: Van Nostrand Reinhold).

Delécolle, R., Maas, S.J., Guérif, M. and Baret, F., 1992, Remote sensing and crop production models: present trends. *ISPRS Journal of Photogrammetry and Remote Sensing*, **47**, pp. 145–161.

Dente, L., Satalino, G., Mattia, F. and Rinaldi, M., 2008, Assimilation of leaf area index derived from ASAR and MERIS data into CERES–Wheat model to map wheat yield. *Remote Sensing of Environment*, **112**, pp. 1395–1407.

De Wit, A.J.W., 1999, The application of a genetic algorithm for crop model steering using NOAA–AVHRR data. In *Proceedings of SPIE Vol. 3868*, E. Zilioli, E.T. Engman and G. Cecchi (Eds), pp. 167–181 (Bellingham, WA: SPIE).

Doraiswamy, P.C., Hatfield, J.L., Jackson, T.J., Akhmedov, B., Prueger, J. and Stern, A., 2004, Crop condition and yield simulation using Landsat and MODIS. *Remote Sensing of Environment*, **92**, pp. 548–559.

Doraiswamy, P.C., Moulin, S., Cook, P.W. and Stern, A., 2003, Crop yield assessment from remote sensing. *Photogrammetric Engineering and Remote Sensing*, **69**, pp. 665–674.

Fang, H. and Liang, S., 2003, Retrieve LAI from Landsat 7 ETM+ data with a neural network method: Simulation and validation study. *IEEE Transactions on Geoscience and Remote Sensing*, **41**, pp. 2052–2062.

Fang, H. and Liang, S., 2005, A hybrid inversion method for mapping leaf area index from MODIS data: Experiments and application to broadleaf and needleleaf canopies. *Remote Sensing of Environment*, **94**, pp. 405–424.

Fang, H., Liang, S., Hoogenboom, G., Teasdale, J. and Cavigelli, M., 2008, Corn yield estimation through assimilation of remote sensed data into the CSM–CERES–Maize model. *International Journal of Remote Sensing*, **29**, pp. 3011–3032.

Fang, H., Liang, S. and Kuusk, A., 2003, Retrieving leaf area index using a genetic algorithm with a canopy radiative transfer model. *Remote Sensing of Environment*, **85**, pp. 257–270.

Gao, X., Huete, A.R. and Didan, K., 2003, Multisensor comparisons and validation of MODIS vegetation indices at the semiarid Jornada Experimental Range. *IEEE Transactions on Geoscience and Remote Sensing*, **41**, pp. 2368–2381.

Goldberg, D.E., 1989, *Genetic Algorithms in Search, Optimization and Machine Learning* (Reading, MA: Addison-Wesley).

Guérif, M. and Duke, C.L., 2000, Adjustment procedures of a crop model to the site specific characteristics of soil and crop using remote sensing data assimilation. *Agriculture, Ecosystems & Environment*, **81**, pp. 57–69.

HOOGENBOOM, G., JONES, J.W., WILKENS, P.W., PORTER, C.H., BATCHELOR, W.D., HUNT, L.A., BOOTE, K.J., SINGH, U., URYASEV, O., BOWEN, W.T., GIJSMAN, A.J., TOIT, A.D., WHITE, J.W. and TSUJI, G.Y., 2004, *Decision Support System for Agrotechnology Transfer Version 4.0* [CD-ROM] (Honolulu, Hawaii: University of Hawaii).

HOOGENBOOM, G., WILKENS, P.W. and TSUJI, G.Y. (Eds), 1999, *Decision Support System for Agrotechnology Transfer, Version 3 Volume 4* (Honolulu, Hawaii: University of Hawaii).

HUETE, A., DIDAN, K., MIURA, T., RODRIGUEZ, E.P., GAO, X. and FERREIRA, L.G., 2002, Overview of the radiometric and biophysical performance of the MODIS vegetation indices. *Remote Sensing of Environment*, **83**, pp. 195–213.

JACQUEMOUD, S., BACOUR, C., POILVE, H. and FRANGI, J.P., 2000, Comparison of four radiative transfer models to simulate plant canopies reflectance-direct and inverse mode. *Remote Sensing of Environment*, **74**, pp. 471–481.

JACQUEMOUD, S. and BARET, F., 1990, PROSPECT: a model of leaf optical properties spectra. *Remote Sensing of Environment*, **34**, pp. 75–91.

JACQUEMOUD, S., USTIN, S.L., VERDEBOUT, J., SCHMUCK, G., ANDREOLI, G. and HOSGOOD, B., 1996, Estimating leaf biochemistry using the PROSPECT leaf optical properties model. *Remote Sensing of Environment*, **56**, pp. 194–202.

JET PROPULSION LABORATORY (JPL), 1998, *Aster Spectral Library, Version 1.2* (Pasadena, CA: Jet Propulsion Laboratory). Available online at http://speclib.jpl.nasa.gov.

JIANG, D., WANG, N.B., YANG, X.H. and WANG, J.H., 2003, Study on the interaction between NDVI profile and the growing status of crops. *Chinese Geographical Science*, **13**, pp. 62–65.

JONES, J.W., HOOGENBOOM, G., PORTER, C.H., BOOTE, K.J., BATCHELOR, W.D., HUNT, L.A., WILKENS, P.W., SINGH, U., GIJSMAN, A.J. and RITCHIE, J.T., 2003, The DSSAT cropping system model. *European Journal of Agronomy*, **18**, pp. 235–265.

JONGSCHAAP, R.E.E., 2006, Run-time calibration of simulation models by integrating remote sensing estimates of leaf area index and canopy nitrogen. *European Journal of Agronomy*, **24**, pp. 316–324.

JUSTICE, C.O., VERMOTE, E., TOWNSHEND, J.R.G., DEFRIES, R., ROY, D.P., HALL, D.K., SALOMONSON, V.V., PRIVETTE, J.L., RIGGS, G., STRAHLER, A., LUCHT, W., MYNENI, R.B., KNYAZIKHIN, Y., RUNNING, S.W., NEMANI, R.R., WAN, Z., HUETE, A.R. and VAN LEEUWEN, W., 1998, The Moderate Resolution Imaging Spectroradiometer (MODIS): land remote sensing for global change research. *IEEE Transactions on Geoscience and Remote Sensing*, **36**, pp. 1228–1249.

KANG, S., RUNNING, S.W., LIM, J.-H., ZHAO, M., PARK, C.-R. and LOEHMAN, R., 2003, A regional phenology model for detecting onset of greenness in temperate mixed forests, Korea: an application of MODIS leaf area index. *Remote Sensing of Environment*, **86**, pp. 232–242.

KIMES, D.S., KNYAZIKHIN, Y., PRIVETTE, J.L., ABUELGASIM, A.A. and GAO, F., 2000, Inversion methods for physically-based models. *Remote Sensing Review*, **18**, pp. 381–440.

KINIRY, J.R., WILLIAMS, J.R., VANDERLIP, R.L., ATWOOD, J.D., REICOSKY, D.C., MULLIKEN, J., COX, W.J., MASCAGNI, H.J.J., HOLLINGER, S.E. and WIEBOLD, W.J., 1997, Evaluation of two maize models for nine U.S. locations. *Agronomy Journal*, **89**, pp. 421–426.

KOGAN, F., YANG, B., GUO, W., PEI, Z. and JIAO, X., 2005, Modelling corn production in China using AVHRR-based vegetation health indices. *International Journal of Remote Sensing*, **26**, pp. 2325–2336.

KUUSK, A., 1998, Monitoring of vegetation parameters on large areas by the inversion of a canopy reflectance model. *International Journal of Remote Sensing*, **19**, pp. 2893–2905.

KUUSK, A., 2001, A two-layer canopy reflectance model. *Journal of Quantitative Spectroscopy and Radiative Transfer*, **71**, pp. 1–9.

KUUSK, A., ANDRIEU, B., CHELLE, M. and ARIES, F., 1997, Validation of a Markov chain canopy reflectance model. *International Journal of Remote Sensing*, **18**, pp. 2125–2146.

LIANG, S., 2004, *Quantitative Remote Sensing of Land Surfaces* (New York: John Wiley and Sons).

Liang, S. and Qin, J., 2008, Data assimilation methods for land surface variable estimation. In *Advances in Land Remote Sensing: System, Modeling, Inversion and Application,* S. Liang (Ed.), pp. 319–339 (New York: Springer).

Lizaso, J.I., Batchelor, W.D. and Adams, S.S., 2001, Alternate approach to improve kernel number calculation in CERES–maize. *Transactions of the ASAE*, **44**, pp. 1011–1018.

Maas, S., 1988a, Using satellite data to improve model estimates of crop yield. *Agronomy Journal*, **80**, pp. 662–665.

Maas, S.J., 1988b, Use of remotely-sensed information in agricultural crop growth models. *Ecological Modeling*, **41**, pp. 247–268.

MacDonald, R. and Hall, F., 1980, Global crop forecasting. *Science*, **208**, pp. 670–679.

Mo, X., Xiang, Y., McVicar, T.R., Liu, S., Lin, Z. and Xu, Y., 2005, Prediction of crop yield, water consumption and water use efficiency with a SVAT-crop growth model using remotely sensed data on the North China Plain. *Ecological Modeling*, **183**, pp. 301–322.

Moulin, S., Bondeau, A. and Delécolle, R., 1998, Combining agricultural crop models and satellite observations: from field to regional scale. *International Journal of Remote Sensing*, **19**, pp. 1021–1036.

Myneni, R.B., Hoffman, S., Knyazikhin, Y., Privette, J.L., Glassy, J., Tian, Y., Wang, Y., Song, X., Zhang, Y., Smith, G.R., Lotsch, A., Friedl, M., Morisette, J.T., Votava, P., Nemani, R.R. and Running, S.W., 2002, Global products of vegetation leaf area and fraction absorbed PAR from year one of MODIS data. *Remote Sensing of Environment*, **83**, pp. 214–231.

O'Neal, M.R., Frankenberger, J.R. and Ess, D.R., 2002, Use of CERES–Maize to study effect of spatial precipitation variability on yield. *Agricultural Systems*, **73**, pp. 205–225.

Plummer, S.E., 2000, Perspectives on combining ecological process models and remotely sensed data. *Ecological Modeling*, **129**, pp. 169–186.

Press, W.H., Teukolsky, S.A., Vetterling, W.T. and Flannery, B.P., 1992, *Numerical Recipes in Fortran 77: The Art of Scientific Computing* (New York: Cambridge University Press).

Price, J.C., 1990, On the information content of soil reflectance spectra. *Remote Sensing of Environment*, **33**, pp. 113–121.

Qin, J., Liang, S., Li, X. and Wang, J., 2008, Development of the adjoint model of a canopy radiative transfer model for sensitivity study and inversion of leaf area index. *IEEE Transactions on Geoscience and Remote Sensing*, **46**, pp. 2028–2037.

Savitzky, A. and Golay, M.J.E., 1964, Smoothing and differentiation of data by simplified least squares procedures. *Analytical Chemistry*, **36**, pp. 1627–1639.

Singh, R., Goyal, R.C., Saha, S.K. and Chhikara, R.S., 1992, Use of satellite spectral data in crop yield estimation surveys. *International Journal of Remote Sensing*, **14**, pp. 2583–2592.

Thenkabail, P.S., Ward, A.D., Lyon, J.G. and Van Deventer, P., 1992, Landsat Thematic Mapper indices for evaluating management and growth characteristics of soybeans and corn. *Transactions of the ASAE*, **35**, pp. 1441–1448.

Tojo Soler, C.M., Sentelhas, P.C. and Hoogenboom, G., 2007, Application of the CSM–CERES–Maize model for planting date evaluation and yield forecasting for maize grown off-season in a subtropical environment. *European Journal of Agronomy*, **27**, pp. 165–177.

Tsuji, G.Y., Uehara, G. and Balas, S., 1994, *Decision Support System for Agrotechnology Transfer, Version 3* (Honolulu, Hawaii: University of Hawaii).

Tubiello, F.N., Rosenzweig, C., Kimball, B.A., Pinter, P.J.J., Wall, G.W., Hunsaker, D.J., Lamorte, R.L. and Garcia, R.L., 1999, Testing CERES–wheat with free-air carbon dioxide enrichment (FACE) experiment data: CO2 and water interactions. *Agronomy Journal*, **91**, pp. 247–255.

Weiss, M., Troufleau, D., Baret, F., Chauki, H., Prévot, L., Olioso, A., Bruguier, N. and Brisson, N., 2001, Coupling canopy functioning and radiative transfer models for

remote sensing data assimilation. *Agricultural and Forest Meteorology*, **108**, pp. 113–128.

WEISSTEINER, C.J. and KÜHBAUCH, W., 2005, Regional yield forecasts of malting barley (Hordeum vulgare L.) by NOAA–AVHRR remote sensing data and ancillary data. *Journal of Agronomy and Crop Science*, **191**, pp. 308–320.

XIE, Y., KINIRY, J.R., NEDBALEK, V. and ROSENTHAL, W.D., 2001, Maize and sorghum simulations with CERES–maize, SORKAM, and ALMANAC under water-limiting conditions. *Agronomy Journal*, **93**, pp. 1148–1155.

YANG, H.S., DOBERMANN, A., LINDQUIST, J.L., WALTERS, D.T., ARKEBAUER, T.J. and CASSMAN, K.G., 2004, Hybrid–maize – a maize simulation model that combines two crop modeling approaches. *Field Crops Research*, **87**, pp. 131–154.

ZARCO-TEJADA, P.J., RUEDA, C.A. and USTIN, S.L., 2003, Water content estimation in vegetation with MODIS reflectance data and model inversion methods. *Remote Sensing of Environment*, **85**, pp. 109–124.

ZHANG, X., FRIEDL, M.A., SCHAAF, C.B., STRAHLER, A.H., HODGES, J., GAO, F., REED, B. and HUETE, A., 2003, Monitoring vegetation phenology using MODIS. *Remote Sensing of Environment*, **84**, pp. 471–475.